Journal of Marine Systems xxx (2013) xxx–xxx

Contents lists available at SciVerse ScienceDirect

Journal of Marine Systems

journal homepage: www.elsevier.com/locate/jmarsys

Population-specific shifts in viral and microbial abundance within a cryptic upwelling

James S. Paterson [a,*], Sasi Nayar [b], James G. Mitchell [a], Laurent Seuront [a,b,c]

[a] School of Biological Sciences, Flinders University, GPO Box 2100, Adelaide 5001, South Australia, Australia
[b] South Australian Research and Development Institute, Aquatic Sciences, PO Box 120, Henley Beach 5024, South Australia, Australia
[c] Centre National de la Recherche Scientifique, Laboratoire d'Océanologie et de Géosciences, UMR LOG 8187, Université des Sciences et Technologies de Lille, Station Marine, 62930 Wimereux, France

ARTICLE INFO

Article history:
Received 29 March 2012
Received in revised form 16 December 2012
Accepted 19 December 2012
Available online xxxx

Keywords:
Coastal upwelling
Cryptic
Viruses
Bacteria
Pico-phytoplankton
Flow cytometry

ABSTRACT

Coastal upwelling systems play an essential role in bringing cold and nutrient-rich water into the euphotic zone, hence enhancing the biological productivity of the world's oceans. We describe a "cryptic" upwelling occurring in South Australian waters, in which cold upwelled waters do not reach surface waters and do not exhibit a sea surface temperature (SST) signature. Due to the wide continental shelf (ca. 100 km), upwelled waters form a sub-surface cold water pool and are forced north-west after a secondary event. Using flow cytometry we investigated the abundance and composition of viruses, heterotrophic bacteria and pico-phytoplankton within upwelling affected and unaffected waters. Our results identified the presence of upwelled waters at and below the Deep-Chlorophyll Maximum (DCM), where water temperature was at least 4 °C colder than surface waters. In contrast to previous studies, no significant differences were observed between upwelled and non-upwelled waters for most individual viral, bacterial and pico-phytoplankton sub-groups. However, one viral, one bacterial and two pico-phytoplankton sub-groups were significantly more abundant at the DCM. This indicates the presence of depth- and population-specific shifts in abundance and potential niche partitioning of these cytometrically-defined sub-groups that may be related to their host organisms and/or resource availability.

1. Introduction

Coastal upwelling plays a critical role in enhancing the biological productivity of the world's oceans, bringing nutrient rich water from the deep into the euphotic zone, which leads to high primary productivity and biomass, low diversity and simple food webs (Daneri et al., 2000; Ryther, 1969; Sommer et al., 2002). Coastal upwelling systems are typically located within eastern boundary currents, e.g. the Californian, Humboldt, Canary and Benguela currents, and account for the majority of new production in the ocean (Chavez and Messié, 2009; Messié et al., 2009), up to 25% of global fish production (Mann, 2000) and support major fisheries throughout the world (Alheit and Niquen, 2004; Cushing, 1971; Mann, 2000; Ryther, 1969).

In Australia, where the eastern boundary Leeuwin Current uncharacteristically flows poleward and hence suppresses favourable upwelling conditions (Hanson et al., 2005; Smith et al., 1991), upwelling systems are confined to local areas such as the Capes Current and Gascoyne regions of Western Australia (Gersbach et al., 1999; Hanson et al., 2007), the intrusion and separation points of the East Australian Current from the east coast of Australia (Rochford, 1975; Roughan and Middleton, 2002), and off the Bonney Coast in south-eastern Australia (Bye, 1972; Lewis, 1981; Middleton and Platov, 2003; Rochford, 1977; Schahinger, 1987). Specifically, the Bonney upwelling, located along a northern boundary current (Bye, 1972; Middleton and Cirano, 2002; Middleton and Platov, 2003; Rochford, 1977), is the beginning of a chain of localised upwelling events, collectively referred to as the South Australian upwelling system, which spreads to the north-west over approximately 600 km of coastline (Kämpf et al., 2004; Middleton and Bye, 2007).

The Bonney upwelling is the most studied upwelling in the south-eastern Australian region (Butler et al., 2002; Middleton and Bye, 2007; Middleton and Platov, 2003; Nieblas et al., 2009; Schahinger, 1987). It operates in the austral summer and is driven by the subtropical ridge, a region of high atmospheric pressure that migrates southward over the Great Australian Bight in summer months, producing upwelling favourable south-easterly winds (Rochford, 1977; Schahinger, 1987). However, during the austral winter the subtropical ridge migrates northward over mainland Australia and produces westerly winds favourable for downwelling (Rochford, 1977). Furthermore, the Flinders Current, a northern boundary current flowing westward, favours localised upwelling by assisting in the exchange of ocean and shelf water masses and by raising the thermocline over the continental shelf (Middleton and Cirano, 2002; Middleton and Platov, 2003). The presence of shelf break canyons in the Bonney upwelling region is also thought to assist in the transportation of nutrient rich bottom waters to the surface (Kämpf, 2010; Middleton and Bye, 2007). In contrast, little is still known about the upwelling that occurs south of Kangaroo Island, hereafter referred to as the du Couedic upwelling system, due to the role

* Corresponding author. Tel.: +61 882015182; fax: +61 882013015.
E-mail addresses: james.paterson@flinders.edu.au (J.S. Paterson), sasi.nayar@sa.gov.au (S. Nayar), jim.mitchell@flinders.edu.au (J.G. Mitchell), laurent.seuront@flinders.edu.au (L. Seuront).

0924-7963/$ – see front matter © 2013 Elsevier B.V. All rights reserved.
http://dx.doi.org/10.1016/j.jmarsys.2012.12.009

played by the du Couedic canyon in the movement of upwelled waters onto the shelf (Kämpf, 2010).

In contrast to the narrow shelf of the Bonney upwelling (20 to 50 km), the du Couedic upwelling system is characterised by a wide continental shelf (ca. 100 km) that does not allow upwelled waters to reach the surface (McClatchie et al., 2006). Instead, upwelled waters form a sub-surface cold water pool south of Kangaroo Island that does not exhibit a sea surface temperature signature (Kämpf, 2010; McClatchie et al., 2006; Fig. 1); hence it is referred to as a cryptic upwelling system. Upwelled waters are brought into the Kangaroo Island sub-surface pool *via* an initial upwelling event and are subsequently forced north-west and into surface waters adjacent to the western Eyre Peninsula by a secondary upwelling event (Kämpf, 2010; McClatchie et al., 2006; Middleton and Bye, 2007; van Ruth et al., 2010).

While the physical processes that control the du Couedic upwelling system are becoming increasingly well understood (Kämpf, 2010; McClatchie et al., 2006; Middleton and Platov, 2003; van Ruth et al., 2010), there is still a critical lack of information about the biological processes, particularly viral and heterotrophic bacterial dynamics, which occur within this system. Specifically, this has been limited to the distribution of chlorophyll *a* (McClatchie et al., 2006; van Ruth et al., 2010) and pico-phytoplankton (Seuront et al., 2010; van Dongen-Vogels et al., 2011). The abundance and population dynamics of viruses and heterotrophic bacteria have previously been investigated in the South Australian upwelling system with a specific focus on the Bonney upwelling and its strong SST signature (Paterson et al., 2012). The current study focuses on the potential consequences of the cryptic nature of the du Couedic upwelling on the spatial distribution of viral, heterotrophic bacterial and pico-phytoplankton communities. In this context, the objectives of this study were (i) to describe the main physical properties of the du Couedic upwelling system that typify its cryptic nature, (ii) to assess the spatial distribution of viral, bacterial and pico-phytoplankton communities within a wind-driven "cryptic" coastal upwelling system, (iii) to investigate the physical factors that may influence the abundances of each group and (iv) to assess the potential links between the abundances of these organisms.

2. Materials and methods

2.1. Study site

The du Couedic Canyon is located on the South Australian continental shelf below the south-west tip of Kangaroo Island (Fig. 1A). Sampling was carried out onboard the *RV Southern Surveyor* from the 18th to the 21st February 2008. Sampling stations with bottom depths of approximately 100, 200, 500, 1000 and 1500 m were located along three parallel transects, located to the west, centre and east of the du Couedic canyon axis (Fig. 1B).

2.2. Sampling procedures

Vertical profiles of temperature and salinity were carried out at each station using a Seabird SBE 911 plus CTD, which was fitted with sensors for dissolved oxygen (Aanderaa Optode 3975) and *in vivo* fluorescence (Chelsea AQUAtracka). *In vivo* fluorescence was treated as a proxy of phytoplankton biomass because *in vivo* fluorescence did not decrease in surface waters during the daylight period, indicating the absence of photoinhibition (Falkowski and Kiefer, 1985). Calibration factors were validated before and after each cast by correcting deviations in sensor records (Beattie, 2008). Water samples for viral, bacterial and pico-phytoplankton abundance were collected from surface waters (4 m) and the Deep-Chlorophyll Maximum (DCM), which ranged from 35 to 63 m in shelf and offshore waters, respectively. Triplicate samples for heterotrophic bacteria and viruses, fixed with glutaraldehyde (0.5% final concentration), were transferred into 2 ml cryovials and incubated for 15 min at 4 °C (Brussaard, 2004). Duplicate pico-phytoplankton samples were fixed with paraformaldehyde (2% final concentration) and incubated for 15 min at 4 °C (Marie et al., 1997). Samples were quick frozen in liquid nitrogen, and once in the laboratory stored at −80 °C and analysed within one month of collection. Samples for nutrients were taken in surface waters and at the DCM and were analysed using a flow injection autoanalyser (Lachat QuikChem®). QuikChem methods were followed for nitrate (QuikChem® Method 31-107-04-1-A), silicate (QuikChem® Method 10-114-27-1-A) and phosphate (QuikChem® Method 31-115-01-1-I).

2.3. Flow cytometric analysis

2.3.1. Heterotrophic bacteria and viruses

Heterotrophic bacteria and viruses were identified and enumerated by flow cytometry (FCM) using a FACScanto flow cytometer (Becton Dickinson), with phosphate-buffered saline (PBS) solution as sheath fluid. Triplicate viral and bacterial samples were thawed rapidly and diluted 1:10 with 0.2 μm filtered TE buffer (10 mM Tris, 1 mM EDTA), stained with SYBR-I Green solution (1:20,000 final dilution; Molecular Probes) and incubated in the dark for 10 min at 80 °C (Brussaard,

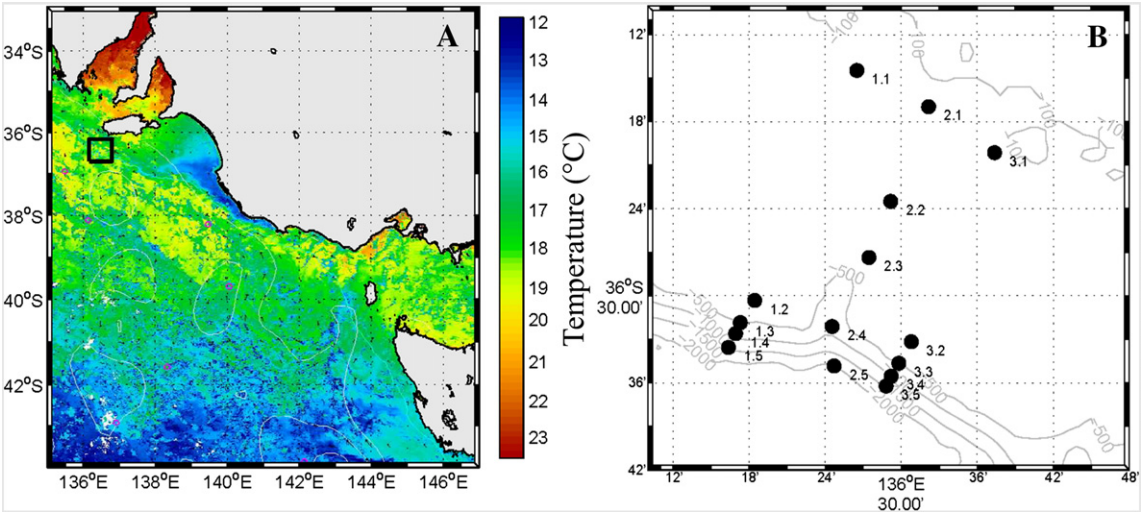

Fig. 1. Sea surface temperature (SST) off south-eastern Australia (A), with the black box indicating the study area (B) with sampling transects and stations located to the west, centre and east of the axis of the du Couedic Canyon. SST data sourced from the Commonwealth Scientific and Industrial Research Organisation (CSIRO; http://www.marine.csiro.au/remotesensing/oceancurrents/).

Please cite this article as: Paterson, J.S., et al., Population-specific shifts in viral and microbial abundance within a cryptic upwelling, J. Mar. Syst. (2013), http://dx.doi.org/10.1016/j.jmarsys.2012.12.009

2004) prior to analysis. Fluorescent beads with a diameter of 1 μm (Molecular Probes) were added to each sample as an internal size and concentration standard at a final concentration of approximately 10^5 beads ml^{-1} (Gasol and del Giorgio, 2000). Forward-angle light scatter (FSC), side-angle light scatter (SSC) and green (SYBR-I) fluorescence were recorded for each sample. WinMDI 2.8 software (© Joseph Trotter) was used to analyse data collected for each sample.

Differences in cell side scatter (SSC) and SYBR Green fluorescence were used to discriminate viral and heterotrophic bacterial sub-groups (Brussaard, 2004; Marie et al., 1997, 1999). Bacterial sub-groups were defined as high DNA (HDNA) and low DNA (LDNA) groups using differences in green fluorescence (Gasol et al., 1999; Li et al., 1995; Fig. 2A, B), while viral sub-groups were partitioned into three groups (VLP1, VLP2 and VLP3) based on their differences in green fluorescence and SSC (Fig. 2A, B).

2.3.2. Pico-phytoplankton

Flow cytometric analysis of pico-phytoplankton samples was done using a FACScanto flow cytometer (Becton Dickinson). Prior to analysis samples were thawed rapidly and 1 μm fluorescent beads (Molecular Probes) were added to each sample as an internal size and concentration standard at a final concentration of approximately 10^5 beads ml^{-1} (Gasol and del Giorgio, 2000). Forward-angle light scatter (FSC), side-angle light scatter (SSC), red (chlorophyll) fluorescence and orange (phycoerythrin) fluorescence were recorded for each sample while phosphate-buffered saline (PBS) solution was used as sheath fluid. WinMDI 2.8 software (© Joseph Trotter) was used to analyse and interpret data for each sample.

Pico-phytoplankton cells were separated into three sub-groups consisting of two cyanobacteria groups (*Synechococcus* sp. and *Prochlorococcus* sp.) and one pico-eukaryotic group based on the observed differences in their red (chlorophyll) and orange (phycoerythrin) fluorescence, and SSC properties (Marie et al., 1997; Fig. 2C, D).

2.4. Stratification index

Potential energy (Φ; J m^{-3}) was calculated for each vertical profile according to Simpson and Bowers (1981). The index Φ indicates how much mechanical energy is required to homogenise a water column. Highly stratified water columns are indicated by high Φ values, while well mixed water columns are indicated by low Φ values (Mann and Lazier, 2006).

2.5. Statistical analysis

Significant relationships between viruses, heterotrophic bacteria and environmental parameters were determined using Pearson's correlation. The determination of significant differences between depths along each transect was done out using the Mann–Whitney *U* test. Multiple comparisons between sampling sites were done using the Kruskal–Wallis test, and a subsequent multiple comparison procedure based on the Tukey's test was used to identify distinct groups of measurements (Zar, 2009).

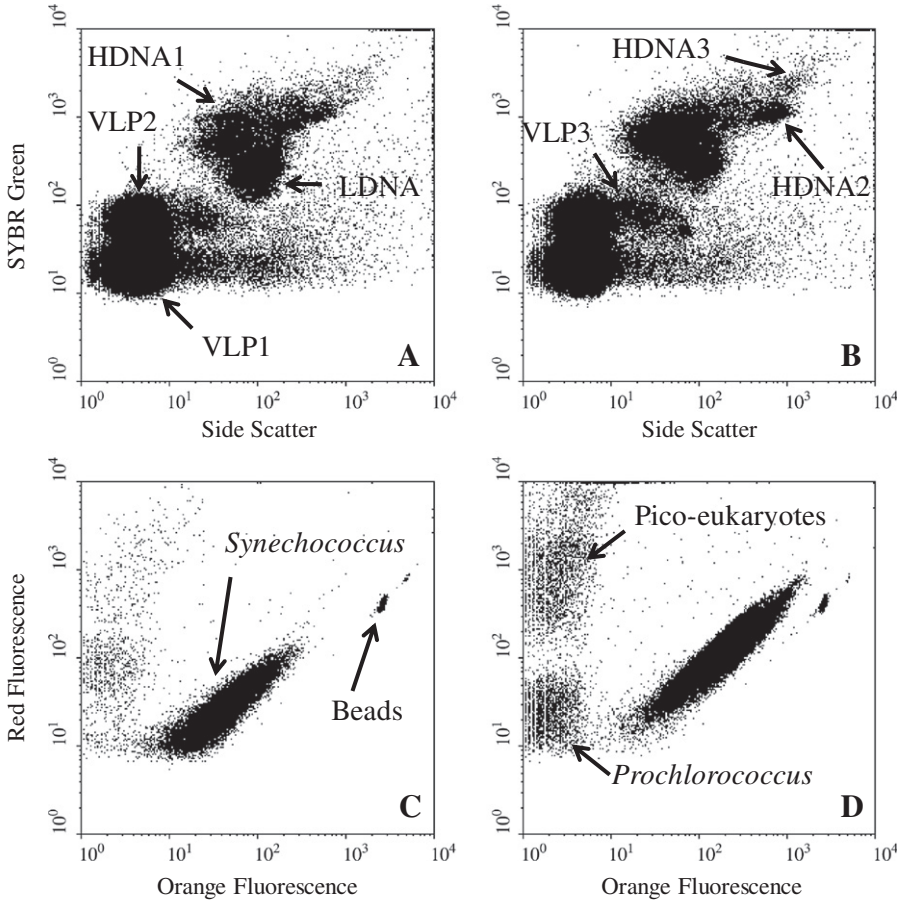

Fig. 2. Representative cytograms used to determine viral and bacterial (A, B; station 2–1) and pico-phytoplankton (C, D; station 2–1) abundance within surface waters (A, C) and at the DCM (B, D).

Please cite this article as: Paterson, J.S., et al., Population-specific shifts in viral and microbial abundance within a cryptic upwelling, J. Mar. Syst. (2013), http://dx.doi.org/10.1016/j.jmarsys.2012.12.009

3. Results

3.1. Environmental parameters

Thermal stratification of the water column was observed in shelf waters (stations 1–1, 2–1 and 3–1) for all three transects. However, the stratification became less defined in slope and offshore waters (Fig. 3). A DCM was also clearly visible in all profiles (Fig. 3). The highest chlorophyll *a* concentration was observed at station 2–1 (0.91 μg l^{-1}; Fig. 3). Sea surface temperatures were at least 4 °C warmer than DCM temperatures over the three shelf stations (stations 1–1, 2–1 and 3–1; Fig. 3). More specifically, temperature at the DCM ranged from 13.7 to 15.7 °C, while the stratification index (Φ; J m^{-3}) was highest at stations located at or near the shelf break, in particular at station 3–2 (125.9 J m^{-3}; Table 1), indicating a stratified water column. Over shelf stations salinity displayed a vertical structure similar to temperature; at all other stations salinity showed little variability over the water column (Fig. 3). This indicates that over shelf stations temperature and salinity are both driving factors in the stratification of the water column, while at all other stations stratification is predominantly temperature driven. Concentrations of nitrate, phosphate and silicate were highest at the DCM over shelf waters along transects 1 and 2 (Table 2). Highest values of nitrate (2.31 μmol l^{-1}), phosphate (0.29 μmol l^{-1}) and silicate (1.06 μmol l^{-1}) were recorded at the DCM at station 1–1, while in surface waters at the same station nitrate (0.00 μmol l^{-1}), phosphate (0.06 μmol l^{-1}) and silicate (0.37 μmol l^{-1}) were lower.

3.2. Viral community

3.2.1. Total viral abundance

Total viral abundance ranged from 6.01×10^5 to 5.64×10^6 ml^{-1} and from 3.18×10^5 to 4.73×10^6 ml^{-1} in surface and DCM waters, respectively (Fig. 4). A 5-fold significant decrease was observed in total viral abundance from shelf to slope waters along transect 2 both in surface waters and at the DCM ($p<0.05$; Fig. 4B), while there was a 3-fold significant increase from slope to offshore waters along transect 3 in surface waters ($p<0.05$; Fig. 4C). No significant differences were observed between depths or transects ($p>0.05$) and no overall trends in total viral abundance were present along any transects ($p>0.05$).

3.2.2. Individual viral sub-group abundance

Three viral sub-groups (VLP1, VLP2, VLP3; Fig. 2A, B) were consistently observed at all stations and depths. VLP1 abundance ranged from 4.26×10^5 to 4.64×10^6 ml^{-1} in surface waters and from 1.99×10^5 to

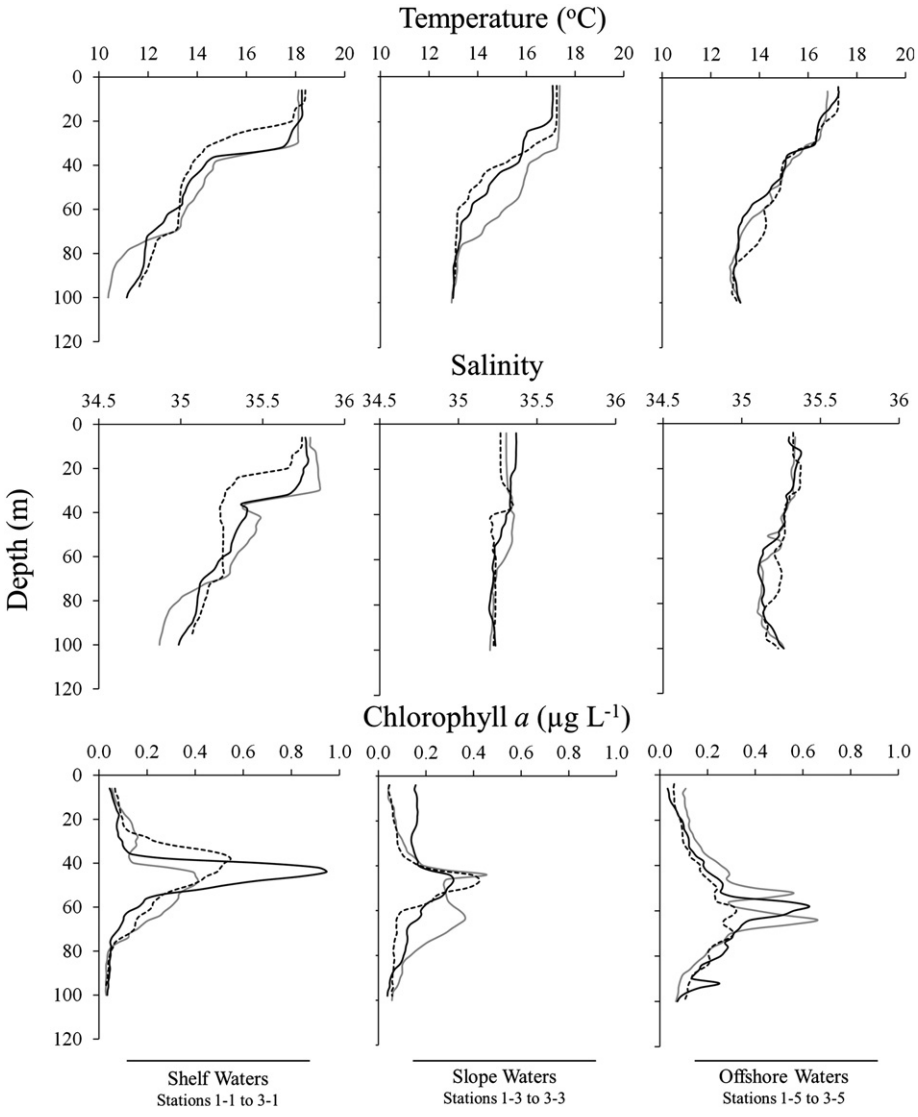

Fig. 3. Vertical profiles of temperature (°C; top panels), salinity (middle panels) and chlorophyll *a* (μg l^{-1}; bottom panels) from CTD casts representative of shelf (stations 1–1 to 3–1), slope (stations 1–3 to 3–3) and offshore (stations 1–5 to 3–5) waters. Grey lines represent stations sampled along transect 1, black lines along transect 2 and dashed lines along transect 3.

Please cite this article as: Paterson, J.S., et al., Population-specific shifts in viral and microbial abundance within a cryptic upwelling, J. Mar. Syst. (2013), http://dx.doi.org/10.1016/j.jmarsys.2012.12.009

Table 1
Potential energy values (J m^{-3}) representing each individual station along the three transects.

	Station				
	1	2	3	4	5
Transect 1	108.1	118.9	117.0	97.5	93.7
Transect 2	113.3	89.3	101.2	113.0	95.0
Transect 3	106.0	124.9	117.5	90.5	98.1

3.85×10^6 ml^{-1} at the DCM. There were no significant differences in VLP1 abundance between depths or transects ($p>0.05$). VLP2 abundance ranged from 1.17×10^5 to 1.23×10^6 ml^{-1} in surface waters and from 4.51×10^4 to 1.48×10^6 ml^{-1} at the DCM. VLP2 abundance displayed no significant differences between depths or transects ($p>0.05$). VLP3 abundance ranged from 3.20×10^4 to 1.29×10^5 ml^{-1} and from 4.12×10^4 to 1.75×10^5 ml^{-1} respectively in surface waters and at the DCM. VLP3 abundance was significantly greater at the DCM than in surface waters along transect 1 ($p<0.05$) and transect 3 ($p<0.01$); no significant difference was observed along transect 2 ($p>0.05$). There were no significant differences in VLP3 abundance between the transects ($p>0.05$). Along transect 2 in both surface and DCM waters VLP1 and VLP2 significantly decreased ($p<0.05$) from shelf to slope waters. However, no overall trends in VLP1, VLP2 and VLP3 abundance were present along any of the three transects ($p>0.05$).

3.2.3. Viral community composition

Viral community composition was dominated by VLP1, which represented respectively up to 82% and 80% of total viral abundance in surface and DCM waters (Fig. 5A–C). The highest values of VLP1 were recorded at stations 2–1 and 3–1 in surface waters. VLP2 represented up to 30% and 32% respectively of total viral abundance in surface and DCM waters (Fig. 5A–C). The contribution of VLP3 at the DCM increased from 2% to 19% along transect 2 from shelf to slope waters (Fig. 5B), while also increasing from 2% to 16% along transect 3 (Fig. 5C). However, this was due to a one order of magnitude decrease in VLP1 and VLP2 abundance between shelf and slope waters along both transects.

3.3. Bacterial community

3.3.1. Total bacterial abundance

Total bacterial abundance ranged from 2.15×10^5 to 9.89×10^5 cells ml^{-1} and from 3.12×10^5 to 1.09×10^6 cells ml^{-1} in surface and DCM waters, respectively (Fig. 4). No significant differences were observed between depths or transects ($p>0.05$), and no overall trends were visible along any transect at both depths ($p>0.05$).

3.3.2. Individual bacterial sub-group abundance

Three bacterial sub-groups (LDNA, HDNA1, HDNA2; Fig. 2A, B) were observed at all stations and depths. In contrast, one sub-group (HDNA3) was only present at four stations along transects 2 and 3 and at the DCM only (Fig. 2A, B). HDNA3 was the largest bacterial sub-group (i.e. highest nucleic acid content and cell side scatter) identified. This sub-group was not considered to be heterotrophic flagellates (size ca. 2–5 μm) due to the cells' smaller size relative to the 1 μm fluorescent beads added as an internal size standard, and the sub-group position on the cytogram (Christaki et al., 2011; Zubkov et al., 2007). LDNA abundance ranged from 9.31×10^4 to 5.88×10^5 cells ml^{-1} in surface waters and from 1.37×10^5 to 6.15×10^5 cells ml^{-1} at the DCM. LDNA abundance showed no significant differences between depths or transects ($p>0.05$). HDNA1 abundance ranged from 6.88×10^4 to 3.24×10^5 cells ml^{-1} in surface waters and from 9.73×10^4 to 6.96×10^5 cells ml^{-1} at the DCM. HDNA1 abundance was significantly greater at the DCM than in surface waters along transect 3 ($p<0.05$); no significant differences were observed between transects ($p>0.05$). HDNA2 abundance ranged from 3.47×10^3 to 1.62×10^5 cells ml^{-1} in surface waters and from 1.53×10^3 to 1.07×10^5 cells ml^{-1} at the DCM. There were no significant differences between depths or transects ($p>0.05$) for HDNA2 abundance. HDNA3 abundance ranged from 4.73×10^3 to 4.12×10^4 cells ml^{-1} at the DCM only. There were no significant differences between transects ($p>0.05$). No overall trends in LDNA, HDNA1, HDNA2 and HDNA3 were present along any of the three transects ($p>0.05$).

3.3.3. Bacterial community composition

LDNA bacteria dominated the community composition, contributing up to 69% in both surface and DCM waters (Fig. 5D–F). Along transect 3 HDNA2 decreased from 21% to 1% and from 18% to 2% from shelf to slope stations in surface and DCM waters, respectively (Fig. 5F). HDNA3 represented up to 8.7% of total bacterial abundance (Fig. 5E, F).

3.4. Pico-phytoplankton community

Synechococcus ranged from 8.83×10^4 to 6.50×10^6 cells ml^{-1} and from 4.18×10^4 to 4.89×10^6 cells ml^{-1} in surface and DCM waters, respectively. *Synechococcus* abundance showed no significant differences between depths or transects ($p>0.05$), and no trends were present along any transects ($p>0.05$). *Prochlorococcus* abundance ranged from 2.83×10^3 to 6.38×10^4 cells ml^{-1} in surface waters and from 1.30×10^4 to 2.30×10^5 cells ml^{-1} at the DCM. *Prochlorococcus* was significantly more abundant at the DCM than in surface waters along transect 1 ($p<0.01$; Fig. 6D) and transect 2 ($p<0.05$; Fig. 6E). *Prochlorococcus* abundance significantly decreased along transect 2 in surface waters ($p<0.05$; Fig. 6E), while no trends were present at the DCM ($p>0.05$). Although no significant trends were detected along transects 1 and 3 at both depths ($p>0.05$), *Prochlorococcus* abundance was greater at offshore stations along transect 1 and at inshore stations along transect 3 in DCM waters (Fig. 6D, F). Pico-eukaryote abundance ranged 4.44×10^2 to 2.92×10^4 cells ml^{-1} in surface waters and from 6.61×10^3 to 2.65×10^5 cells ml^{-1} at the DCM. Pico-eukaryote abundance was significantly greater at the DCM than in surface waters along transect 1 ($p<0.01$; Fig. 6G) and transect 2 ($p<0.05$; Fig. 6H); no significant differences were observed between transects ($p>0.05$). No trends in pico-eukaryote abundance were present along any of the three transects ($p>0.05$).

Table 2
Nutrient concentrations within surface and deep-chlorophyll max (DCM) waters at each station along the three shelf to offshore transects.

		Station														
		1			2			3			4			5		
		NO_3^-	PO_4^{3-}	SiO_2	NO_3^-	PO_4^{3-}	SiO_2	NO_3^-	PO_4^{3-}	SiO_2	NO_3^-	PO_4^{3-}	SiO_2	NO_3^-	PO_4^{3-}	SiO_2
Transect 1	Surface	0.00	0.06	0.37	0.02	0.15	0.05	0.03	0.18	0.06	0.00	0.15	0.09	0.03	0.14	0.09
	DCM	2.31	0.29	1.06	0.42	0.22	0.04	0.03	0.12	0.02	0.26	0.26	0.00	1.32	0.27	0.19
Transect 2	Surface	0.00	0.10	0.35	0.00	0.05	0.07	0.02	0.07	0.08	0.00	0.15	0.07	0.02	0.12	0.06
	DCM	1.75	0.26	0.77	–	–	–	0.69	0.22	0.10	0.38	0.19	0.03	–	–	–
Transect 3	Surface	0.00	0.05	0.31	–	–	–	0.00	0.19	0.05	0.00	0.16	0.07	0.02	0.15	0.10
	DCM	0.13	0.10	0.07	–	–	–	0.13	0.23	0.08	0.11	0.16	0.00	0.36	0.19	0.03

Please cite this article as: Paterson, J.S., et al., Population-specific shifts in viral and microbial abundance within a cryptic upwelling, J. Mar. Syst. (2013), http://dx.doi.org/10.1016/j.jmarsys.2012.12.009

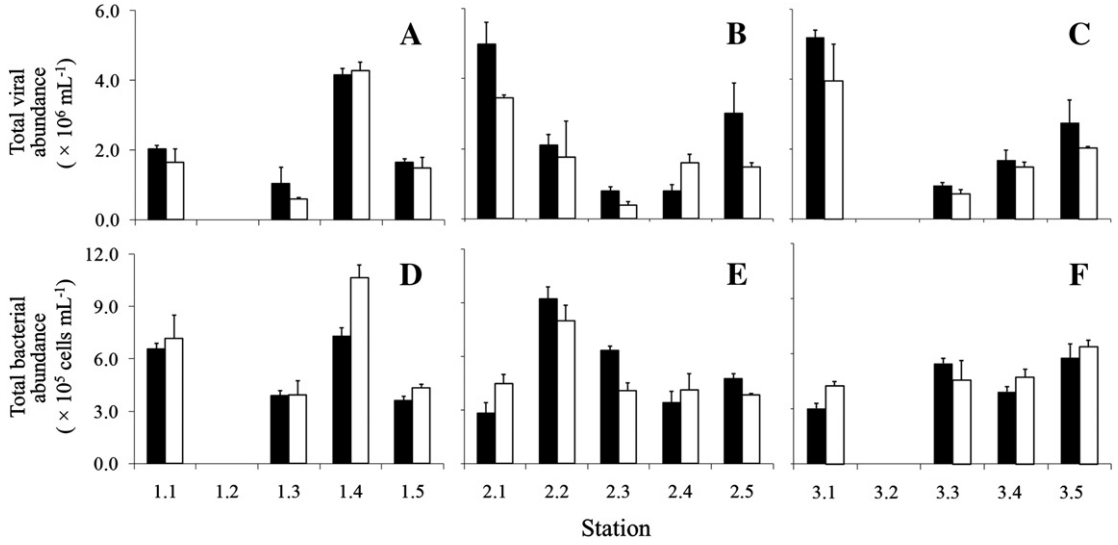

Fig. 4. Total viral (A, B, C) and heterotrophic bacterial (D, E, F) abundance within surface waters (black bars) and the DCM (white bars) along the west (1–1 to 1–5), centre (2–1 to 2–5) and east (3–1 to 3–5) transects of the du Couedic Canyon. Error bars represent standard deviation of the mean.

Synechococcus dominated the composition of pico-phytoplankton abundance, contributing up to 98.5% and 94% of total abundance in surface waters and the DCM, respectively. *Prochlorococcus* represented up to 18% and 45% of total pico-phytoplankton abundance respectively in surface waters and at the DCM. In contrast, pico-eukaryote abundance represented up to 1.5% and 13.5% of pico-phytoplankton abundance in surface waters and at the DCM, respectively.

4. Discussion

4.1. Evidence for a cryptic upwelling

Surface water temperatures at shelf stations (18.1 to 18.4 °C) were not consistent with the signature of upwelled waters from typical upwelling systems (Fig. 1A). However, at the DCM water

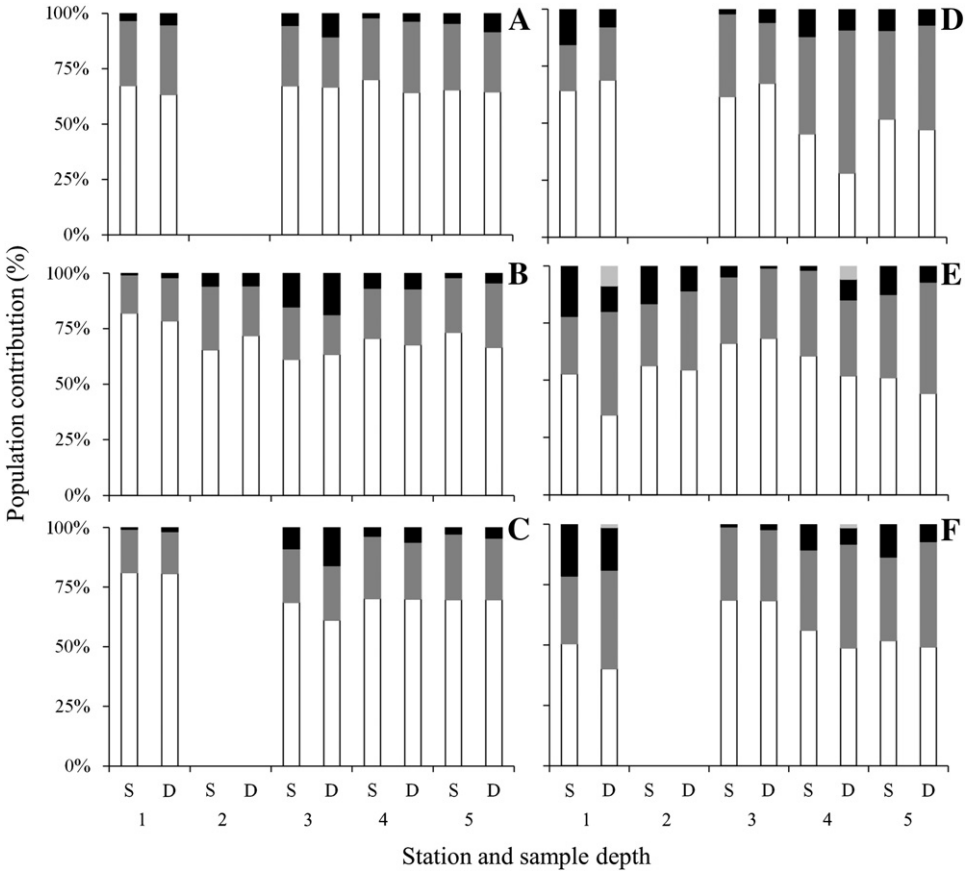

Fig. 5. Community composition of viruses (A, B, C) and heterotrophic bacteria (D, E, F). White bars represent VLP1 (A, B, C) and LDNA (D, E, F), dark grey bars VLP2 (A, B, C) and HDNA1 (D, E, F), black bars VLP3 (A, B, C) and HDNA2 (D, E, F), and light grey bars HDNA3 (D, E, F). Plots A and D represent transect 1, B and E represent transect 2, and C and F represent transect 3. Depths sampled are surface waters (S) and the DCM (D).

Please cite this article as: Paterson, J.S., et al., Population-specific shifts in viral and microbial abundance within a cryptic upwelling, J. Mar. Syst. (2013), http://dx.doi.org/10.1016/j.jmarsys.2012.12.009

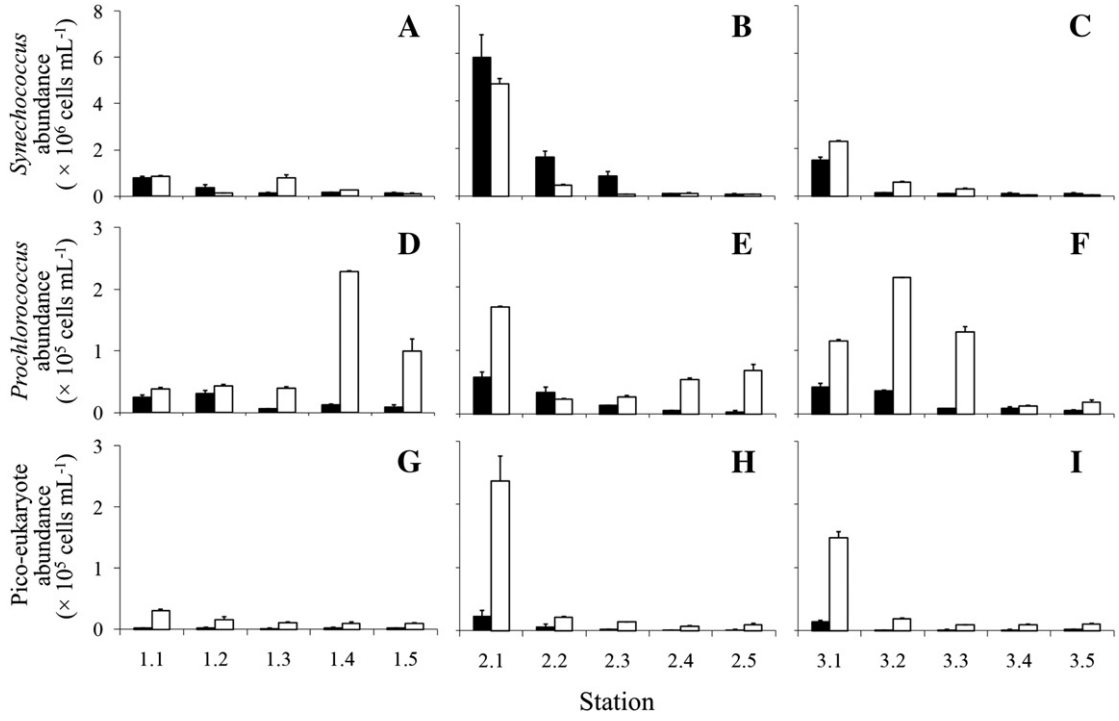

Fig. 6. Abundance of *Synechococcus* (A, B, C), *Prochlorococcus* (D, E, F) and pico-eukaryotes (G, H, I) within surface waters (black bars) and the DCM (white bars) along the west (1–1 to 1–5), centre (2–1 to 2–5) and east (3–1 to 3–5) transects of the du Couedic Canyon. Error bars represent standard deviation of the mean.

temperature ranged from 14.0 to 14.4 °C, and from 10.3 to 11.6 °C at 100 m depth (Fig. 3), suggesting the presence of upwelled waters at and below the DCM. Thermal stratification of the water column was present over shelf waters at all three stations, and was most defined at stations 1–1 and 1–2 (Fig. 3). These observations are consistent with previous studies conducted in this region showing that upwelled waters do not reach the surface but form a sub-surface cold water pool after an initial wind-driven upwelling event (Kämpf, 2010; McClatchie et al., 2006; Middleton and Platov, 2003; van Ruth et al., 2010). Furthermore, the concentrations of nitrate, silicate and phosphate were the highest at the DCM along transects 1 and 2 within shelf waters (stations 1–1 and 2–1; Table 2), hence also indicating the presence of upwelled waters at the DCM. Our observations indicate that two separate and distinct water masses were present over shelf stations (stations 1–1 to 3–1 and 1–2 to 3–2) in the form of surface waters, exhibiting the typical properties of temperate surface water environments, and the DCM which was influenced by upwelled waters (Fig. 3).

These results contrast to a nearby wind-driven coastal upwelling system, the Bonney upwelling, in which nutrient rich upwelled waters are driven to the surface and are clearly visible on SST images (Rochford, 1977; Schahinger, 1987). This is due to the narrow (20 to 50 km) continental shelf where the core of the upwelling lies (Middleton and Bye, 2007). Unlike the du Couedic upwelling which lies over a much wider (ca. 100 km) continental shelf, the Bonney system displays no separation of water masses and upwelled waters are visible throughout the whole water column (Paterson et al., 2012). Similar observations have been made within the highly productive Californian, Benguela, Humboldt and Canary upwelling systems (Chavez and Messié, 2009; Messié et al., 2009), where clear upwelling signatures are consistently present in surface waters and throughout the whole water column. The current study has hence further highlighted the cryptic nature of the du Couedic upwelling and provided a more detailed understanding of the physical properties of this system.

4.2. Nutrient availability controls specific viral sub-group abundance

Total viral abundance observed within the du Couedic upwelling system was approximately one order of magnitude lower than values recorded in two previous studies conducted in upwelling systems (Eissler et al., 2010; He et al., 2009). We observed no significant difference in total viral abundance between upwelling affected DCM waters and unaffected surface waters (Fig. 4A–C). In classical upwelling systems where upwelled waters reach the surface layer, total viral abundance is the highest in surface waters and decreases with depth (Eissler et al., 2010; He et al., 2009). However, to our knowledge, only one study has investigated the abundance and dynamics of cytometrically-defined viral sub-groups within an upwelling system (Paterson et al., 2012). The identification of viral sub-groups provides information on the potential role they play (i.e. infecting bacteria or phytoplankton cells) and distinct dynamics they exhibit, which have been overlooked in previous upwelling studies dealing only with total viral abundance (Eissler et al., 2010; He et al., 2009).

Three individual viral sub-groups (VLP1, VLP2, VLP3; Fig. 2) were present in both surface and DCM waters. We observed no more than a 2-fold difference in VLP1, VLP2 and VLP3 abundance between the two depths sampled. This contrasts to a previous study that observed (i) up to four individual viral sub-groups and (ii) up to 10-fold changes in viral sub-group abundance between upwelled and non-upwelled waters (Paterson et al., 2012). The observed differences may be related to nutrient availability. Specifically, increased levels of phosphorus stimulate viral production (Lymer and Vrede, 2006), while low nutrient availability to host organisms may lead to a reduction in burst size (Middelboe, 2000; Weinbauer, 2004). The higher concentrations of nitrate and phosphate in upwelled than in non-upwelled waters during the present study are consistent with previous observations in upwelling systems (Figueiras et al., 2006; Longnecker et al., 2005; Paterson et al., 2012). However, we found no significant difference in VLP1 and VLP2 abundance between the two different water masses. We also observed no significant differences in individual bacterial sub-group

Please cite this article as: Paterson, J.S., et al., Population-specific shifts in viral and microbial abundance within a cryptic upwelling, J. Mar. Syst. (2013), http://dx.doi.org/10.1016/j.jmarsys.2012.12.009

(LDNA and HDNA2) abundances between the two depths, suggesting the concentration of nitrate and phosphate may not be the main factor controlling the potential hosts of these viral sub-groups. In contrast to VLP1 and VLP2 abundance, we observed significantly greater VLP3 abundance at the DCM than in surface waters along transect 1 ($p<0.05$) and transect 3 ($p<0.01$). High levels of nitrate, phosphate (Table 2) and *Prochlorococcus* and pico-eukaryote abundance (Fig. 6) were also observed at the DCM along these transects. This suggests that (i) the high levels of nitrate and phosphate may stimulate the growth of *Prochlorococcus* and pico-eukaryote abundance and (ii) VLP3 may be a phytoplankton infecting viral sub-group. This is congruent with previous studies, which classified a viral sub-group with a flow cytometric signature similar to our VLP3 as a phytoplankton infecting viral sub-group (Baudoux and Brussaard, 2005; Brussaard et al., 1999, 2005, 2008; Larsen et al., 2008). Our observations are also consistent with previous work that has reported a decrease in the abundance of a VLP3-like sub-group from upwelling to non-upwelling conditions (Paterson et al., 2012). However, no significant relationships between VLP3 and any pico-phytoplankton sub-groups were observed along any transect or depth ($p>0.05$).

Our results suggest that individual viral sub-groups may exhibit their own intrinsic characteristics related to their host organisms. However, the dichotomy between bacteriophages (VLP1, VLP2) and phytoplankton viruses (VLP3) based solely on flow cytometric properties may still be too coarse to classify viral sub-groups as it is based on only size and nucleic acid content (Larsen et al., 2008). Further investigation using cell sorting and molecular techniques is hence required to explicitly classify these sub-groups to obtain a clearer understanding of their structure and dynamics.

4.3. Bacterial sub-groups occupy distinct environmental niches

Total bacterial abundances observed in the present work are consistent with previous studies conducted in upwelling-influenced systems (Alonso-Sáez et al., 2007b; Baltar et al., 2007; Cuevas et al., 2004; Figueiras et al., 2006; Longnecker et al., 2005). However, the non-significant differences in bacterial abundance between surface waters and the DCM (Fig. 4D–F) contrast with previously reported decreases in total bacterial abundance from upwelled to non-upwelled waters (Alonso-Sáez et al., 2007b; Baltar et al., 2007; Cuevas et al., 2004). While the abundance of heterotrophic bacteria within upwelling systems is well documented (Cuevas et al., 2004; Figueiras et al., 2006; Troncoso et al., 2003), limited studies have considered flow cytometrically defined heterotrophic bacterial sub-groups (Baltar et al., 2007; Longnecker et al., 2005; Paterson et al., 2012; Sherr et al., 2005). Specifically, sub-groups characterised by a low DNA content have been suggested to be either inactive or dormant cells, while sub-groups with high DNA content represent highly active cells (Gasol et al., 1999; Lebaron et al., 2001; Li et al., 1995; Servais et al., 2003). However, this has recently been challenged (Bouvier et al., 2007; Longnecker et al., 2005; Wang et al., 2009; Zubkov et al., 2001) as LDNA cells may also be active (Bouvier et al., 2007) and retain their small size throughout their growth cycle (Wang et al., 2009). In addition, LDNA cells, while still having lower metabolic activities than HDNA cells, may play a greater role in heterotrophic processes than HDNA cells in eutrophic systems (Longnecker et al., 2005). Individual sub-groups of heterotrophic bacteria may hence perform distinct roles in biogeochemical cycles and ecological processes; however these functions may change with varying conditions (Bouvier et al., 2007). Therefore, the investigation of their abundance and dynamics is essential in understanding their roles within highly productive upwelling systems.

Four heterotrophic bacterial sub-groups were identified (LDNA, HDNA1, HDNA2 and HDNA3) within the du Couedic upwelling system. One sub-group was observed at the DCM only (HDNA3), while all other sub-groups were seen at both depths. No more than a 2-fold difference in LDNA, HDNA1 and HDNA2 abundance was observed between the two depths. This sharply contrasts to observations of up to an 18-fold change in individual bacterial sub-group abundance between upwelling and non-upwelling conditions (Paterson et al., 2012). However, our observation of significantly higher HDNA1 abundance ($p<0.05$) within upwelled waters is consistent with previous studies (Longnecker et al., 2005; Paterson et al., 2012; Sherr et al., 2005). Furthermore, HDNA1 was positively correlated to total viral abundance, *Prochlorococcus* abundance and standing stock of chlorophyll *a* ($p<0.05$) at the DCM along transects 1 and 3, while also observing elevated levels of nitrate and phosphate (Table 2). Environmental factors such as temperature and chlorophyll *a* concentration may influence the composition of bacterial sub-groups (Alonso-Sáez et al., 2007a; Longnecker et al., 2005) and exhibit their own environmental niche (Paterson et al., 2012). Specifically, LDNA cells have been observed to exhibit higher growth rates in waters with low chlorophyll *a* concentration compared with waters with high concentration (Longnecker et al., 2005). Higher HDNA1 abundance at the DCM, where elevated levels of nitrate and phosphate were observed, suggests this sub-group may be better adapted to nutrient rich waters. In contrast, no significant differences were observed in LDNA and HDNA2 abundance between surface waters and the DCM. As a consequence, it is suggested that the driving factors controlling LDNA and HDNA2 abundance within the du Couedic upwelling system are likely to be top-down processes (grazing and viral lysis) rather than bottom-up processes (nutrient and dissolved organic matter). However, further work is needed to (i) specifically identify the taxonomic composition of these individual sub-groups and (ii) ascertain the mechanisms that control heterotrophic bacterial abundance within this system.

4.4. Unusually high virus–bacteria ratio values under non-upwelling conditions

High virus–bacteria ratio (VBR) values generally typify productive and nutrient rich waters (Weinbauer, 2004; Wommack and Colwell, 2000). However, we found VBR values higher in nutrient poor surface waters than at the nutrient rich DCM at shelf stations 2–1 (17.94 to 7.79) and 3–1 (17.37 to 9.42). Furthermore, we observed low levels of nutrient concentrations (Table 2) and pico-phytoplankton abundance (Fig. 6) where high VBR values were present. In addition, at stations 1–1 to 3–1 total viral abundance and total bacterial abundance were respectively higher and lower in surface waters than at the DCM. The decay of viruses due to UV-B radiation, particularly in surface waters, is well known (Suttle and Chen, 1992; Winter et al., 2004). However, we observed no decrease in *in vivo* fluorescence in surface waters and stations that were sampled during the day (i.e. 4 out of 15) displayed no decay in viral abundance at the surface. This suggests the decay of viruses due to UV-B radiation was minimal during the current study. Our results are consistent with a recent study showing an increase in VBR values from eutrophic to oligotrophic conditions, suggesting a possible short persistence of viruses and weak viral processes within productive waters (Paterson et al., 2012). Observations from the present study and recent findings (Paterson et al., 2012) provide a novel understanding of viral abundances, particularly low VBR values within nutrient rich upwelled waters, within temperate upwelling systems.

4.5. Depth-specific pico-phytoplankton sub-group abundance

The abundance and composition of pico-phytoplankton sub-groups appear to be both depth- and population-specific. The abundance of *Synechococcus* did not significantly differ between the DCM and surface waters ($p>0.05$). However, *Prochlorococcus* and pico-eukaryote abundance were observed to be significantly greater at the DCM than in surface waters ($p<0.05$; Fig. 6). High concentrations of phosphate, nitrate and chlorophyll *a* at the DCM may account for the observed increases in abundance of *Prochlorococcus* and pico-eukaryotes. A previous study within South Australian shelf waters (van Dongen-Vogels et al., 2011) also observed high *Prochlorococcus* and pico-eukaryote abundance at

Please cite this article as: Paterson, J.S., et al., Population-specific shifts in viral and microbial abundance within a cryptic upwelling, J. Mar. Syst. (2013), http://dx.doi.org/10.1016/j.jmarsys.2012.12.009

the DCM, particularly during periods of upwelling. However, these observations contrast with previous studies conducted within classical coastal upwelling systems, which observed low *Prochlorococcus* and pico-eukaryote abundances within upwelled waters (Echevarría et al., 2009; Sherr et al., 2005). Hence, our results may be the result of the physical attributes related to this "cryptic" upwelling, potentially affecting the biological processes occurring within the system. Furthermore, *Synechococcus* abundance was the highest in surface waters over shelf station 2–1 (5.85×10^6 cells ml^{-1}; Fig. 6B), a station where low levels of chlorophyll *a* (0.04 μg l^{-1}), phosphate (0.10 μmol l^{-1}) and nitrate (below detection limit) were observed. A recent study has suggested that the growth and abundance of *Synechococcus* may depend on the viral lysis of heterotrophic bacteria (Weinbauer et al., 2011). This is consistent with our observations of high levels of viral and *Synechococcus* abundance and low levels of heterotrophic bacterial abundance in surface waters at station 2–1 (Fig. 4, 6B). While the resolution of the role of viral lysis in driving the dynamic of both heterotrophic bacteria and pico-phytoplankton goes far beyond the objectives of the present work, our results show that pico-phytoplankton, specifically *Prochlorococcus* and pico-eukaryote, abundance within the du Couedic upwelling system is unique and requires further investigation to gain a stronger understanding of their role within this system.

5. Conclusion

The existence of cold upwelled waters at the DCM and the lack of an upwelling signature in the surface waters over the du Couedic Canyon have confirmed previous evidence of the Kangaroo Island sub-surface cold water pool (Kämpf, 2010; McClatchie et al., 2006; Middleton and Platov, 2003; van Ruth et al., 2010), hence the cryptic character of this upwelling system. We have also investigated the presence and distribution of flow cytometrically-defined viral, heterotrophic bacterial and pico-phytoplankton abundance within this system. Although we observed two distinct water masses possessing different physical characteristics, total viral and bacterial abundance did not significantly change between the two water masses. However, one viral and two bacterial sub-groups showed selectivity in their choice of most favourable conditions, while other sub-groups showed no preference between the two water masses. Furthermore, *Prochlorococcus* and pico-eukaryote abundance was significantly greater within upwelling affected DCM waters than at the surface. This may indicate a possible niche partitioning of these cytometrically defined sub-groups. However, due to the extremely complex dynamics of these cytometrically-defined sub-groups, further investigation is required to understand the structure and functional diversity they present.

Acknowledgements

We thank the Captain and crew of the *RV Southern Surveyor*, and to the cruise leader Dr. David Currie for their assistance. This project was funded by the South Australian Government (through the Marine Innovation South Australia initiative) and the Australian Federal Government. This research was also supported under Australian Research Council's Discovery Projects funding scheme (projects number DP0664681 and DP0988554). Professor Seuront is the recipient of an Australian Professorial Fellowship (project number DP0988554). James Paterson is the recipient of a Flinders University Research Scholarship (FURS).

References

Alheit, J., Niquen, M., 2004. Regime shifts in the Humboldt Current ecosystem. Prog. Oceanogr. 60, 201–222.

Alonso-Sáez, L., Arístegui, J., Pinhassi, J., Gómez-Consarnau, L., González, J.M., Vaqué, D., Agustí, S., Gasol, J.M., 2007a. Bacterial assemblage structure and carbon metabolism along a productivity gradient in the NE Atlantic Ocean. Aquat. Microb. Ecol. 46, 43–53.

Alonso-Sáez, L., Gasol, J.M., Aristegui, J., Vilas, J.C., Vaqué, D., Duarte, C.M., Agusti, S., 2007b. Large-scale variability in surface bacterial carbon demand and growth efficiency in the subtropical northeast Atlantic Ocean. Limnol. Oceanogr. 52, 533–546.

Baltar, F., Arístegui, J., Gasol, J.M., Hernández-León, S., Herndl, G.J., 2007. Strong coast–ocean and surface–depth gradients in prokaryotic assemblage structure and activity in a coastal transition zone region. Aquat. Microb. Ecol. 50, 63–74.

Baudoux, A.C., Brussaard, C.P.D., 2005. Characterization of different viruses infecting the marine harmful algal bloom species *Phaeocystis globosa*. Virology 341, 80–90.

Beattie, R.D., 2008. CTD Processing Notes for RV Southern Surveyor Voyage SS02/2008. CSIRO Division of Marine and Atmospheric Research. (available at http://www.marine.csiro.au/datacentre/process/data_files/ss200802/doc/ss200802ctd.pdf [Accessed 22 July 2011]).

Bouvier, T., del Giorgio, P.A., Gasol, J.M., 2007. A comparative study of the cytometric characteristics of high and low nucleic-acid bacterioplankton cells from different aquatic ecosystems. Environ. Microbiol. 9, 2050–2066.

Brussaard, C.P.D., 2004. Optimisation of procedures for counting viruses by flow cytometry. Appl. Environ. Microbiol. 70, 1506–1513.

Brussaard, C.P.D., Thyrhaug, R., Marie, D., Bratbak, G., 1999. Flow cytometric analyses of viral infection in two marine phytoplankton species, *Micromonas pusilla* (Prasinophyceae) and *Phaeocystis pouchetii* (Prymnesiophyceae). J. Phycol. 35, 941–948.

Brussaard, C.P.D., Kuipers, B., Veldhuis, M.J.W., 2005. A mesocosm study of *Phaeocytis globosa* population dynamics I. Regulatory role of viruses in bloom culture. Harmful Algae 4, 859–874.

Brussaard, C.P.D., Timmermans, K.R., Uitz, J., Veldhuis, M.J.W., 2008. Virioplankton dynamics and virally induced phytoplankton lysis versus microzooplankton grazing southeast of the Kerguelen (Southern Ocean). Deep-Sea Res. II 55, 752–765.

Butler, A., Althaus, F., Furlani, D., Ridgway, K., 2002. Assessment of the Conservation Values of the Bonney Upwelling Area: a Component of the Commonwealth Marine Conservation Assessment Program 2002–2004: Report to Environment Australia. Available from CSIRO Marine Research [Internet]. (http://www.environemt.gov.au/coasts/mpa/publications/pubs/conservation-assessment-bonney.pdf).

Bye, J.A.T., 1972. Ocean circulation South of Australia. In: Hayes, D.E. (Ed.), Antarctic Oceanology II: The Australian–New Zealand Sector, Antarctic Research Series, vol. 19. American Geophysical Union, pp. 95–100.

Chavez, F.P., Messié, M., 2009. A comparison of Eastern Boundary Upwelling Ecosystems. Prog. Oceanogr. 83, 80–96.

Christaki, U., Courties, C., Massana, R., Catala, P., Lebaron, P., Gasol, J.M., Zubkov, M.V., 2011. Optimized routine flow cytometric enumeration of heterotrophic flagellates using SYBR Green I. Limnol. Oceanogr. Methods 9, 329–339.

Cuevas, L.A., Daneri, G., Jacob, B., 2004. Microbial activity and organic carbon flow in the upwelling area off Concepcion (36 S), central Chile. Deep-Sea Res. II 51, 2427–2440.

Cushing, D.H., 1971. Upwelling and production of fish. Adv. Mar. Biol. 9, 255–334.

Daneri, G., Dellarossa, V., Quiñones, R., Jacob, B., Montero, P., Ulloa, O., 2000. Primary production and community respiration in the Humboldt Current System off Chile and associated oceanic areas. Mar. Ecol. Prog. Ser. 197, 41–49.

Echevarría, F., Zabala, L., Corzo, A., 2009. Spatial distribution of autotrophic picoplankton in relation to physical forcings: the Gulf of Cadiz, Strait of Gibraltar and Alboran Sea case study. J. Plankton Res. 31, 1339–1351.

Eissler, Y., Letelier, J., Cuevas, L.A., Morales, C.E., Escribano, R., 2010. The microbial community in the coastal upwelling system off Concepción, Chile, 36°S, 2002–2003 period. Rev. Biol. Mar. Oceanogr. 45, 1–18.

Falkowski, P.G., Kiefer, D.A., 1985. Chlorophyll *a* fluorescence in phytoplankton: relationship to photosynthesis and biomass. J. Plankton Res. 7, 715–731.

Figueiras, F.G., Zdanowski, M.K., Crespo, B.G., 2006. Spatial variability in bacterial abundance and other microbial components in the NW Iberian margin during relaxation of a spring upwelling event. Aquat. Microb. Ecol. 43, 255–266.

Gasol, J.M., del Giorgio, P.A., 2000. Using flow cytometry for counting natural planktonic bacteria and understanding the structure of planktonic bacterial communities. Sci. Mar. 64, 197–224.

Gasol, J.M., Zweifel, U.L., Peters, F., Fuhrman, J.A., Hagström, A., 1999. Significance of size and nucleic acid content heterogeneity as measured by flow cytometry in natural planktonic bacteria. Appl. Environ. Microbiol. 65, 4475–4483.

Gersbach, G.H., Pattiaratchi, C.B., Ivey, G.N., Cresswell, G.R., 1999. Upwelling on the south-west coast of Australia—source of the Capes Current? Cont. Shelf Res. 19, 363–400.

Hanson, C.E., Pattiaratchi, C.B., Waite, A.M., 2005. Seasonal production regimes off south-western Australia: influence of the Capes and Leeuwin Currents on phytoplankton dynamics. Aust. J. Mar. Freshw. Res. 56, 1011–1026.

Hanson, C.E., Waite, A.M., Thompson, P.A., Pattiaratchi, C.B., 2007. Phytoplankton community structure and nitrogen nutrition in Leeuwin Current and coastal waters off the Gascoyne region of Western Australia. Deep-Sea Res. II 54, 902–924.

He, L., Yin, K., Yuan, X., Li, D., Zhang, D., Harrison, P.J., 2009. Spatial distribution of viruses, bacteria and chlorophyll in the northern South China Sea. Aquat. Microb. Ecol. 54, 153–162.

Kämpf, J., 2010. On preconditioning of coastal upwelling in the eastern Great Australian Bight. J. Geophys. Res. 115, C12071.

Kämpf, J., Doubell, M., Griffin, D., Matthews, R.L., Ward, T.M., 2004. Evidence of a large seasonal coastal upwelling system along the southern shelf of Australia. Geophys. Res. Lett. 31, L09310.

Larsen, J.B., Larsen, A., Thyrhaug, R., Bratbak, G., Sandaa, R.A., 2008. Response of marine viral populations to a nutrient induced phytoplankton bloom at different pCO_2 levels. Biogeosciences 5, 523–533.

Lebaron, P., Servais, P., Agogué, H., Courties, C., Joux, F., 2001. Does the high nucleic acid content of individual bacterial cells allow us to discriminate between active cells and inactive cells in aquatic systems? Appl. Environ. Microbiol. 67, 1775–1782.

Lewis, R.K., 1981. Seasonal upwelling along the south-eastern coastline of South Australia. Aust. J. Mar. Freshw. Res. 32, 843–854.
Li, W.K.W., Jellett, J.F., Dickie, P.M., 1995. DNA distributions in planktonic bacteria stained with TOTO or TO-pro. Limnol. Oceanogr. 40, 1485–1495.
Longnecker, K., Sherr, B.F., Sherr, E.B., 2005. Activity and phylogenetic diversity of bacterial cells with high and low nucleic acid content and electron transport system activity in an upwelling ecosystem. Appl. Environ. Microbiol. 71, 7737–7749.
Lymer, D., Vrede, K., 2006. Nutrient additions resulting in phage release and formation of non-nucleoid-containing bacteria. Aquat. Microb. Ecol. 43, 107–112.
Mann, K.H., 2000. Ecology of Coastal Waters, with Implications for Management, second ed. Blackwell Science.
Mann, K.H., Lazier, J.R.N., 2006. Dynamics of Marine Ecosystems: Biological–Physical Interactions in the Oceans, third ed. Blackwell Scientific Publications, Cambridge, MA.
Marie, D., Partensky, F., Jacquet, S., Vaulot, D., 1997. Enumeration and cell cycle analysis of natural populations of marine picoplankton by flow cytometry using the nucleic acid statin SYBR Green I. Appl. Environ. Microbiol. 63, 186–193.
Marie, D., Brussaard, C.P.D., Thyrhaug, R., Bratbak, G., Vaulot, D., 1999. Enumeration of marine viruses in culture and natural samples by flow cytometry. Appl. Environ. Microbiol. 65, 45–52.
McClatchie, S., Middleton, J.F., Ward, T.M., 2006. Water mass analysis and alongshore variation in upwelling intensity in the eastern Great Australian Bight. J. Geophys. Res. 111, C08007. http://dx.doi.org/10.1029/2004JC002699.
Messié, M., Ledesma, J., Kolber, D.D., Michisaki, R.P., Foley, D.G., Chavez, F.P., 2009. Potential new production estimates in four eastern boundary upwelling ecosystems. Prog. Oceanogr. 83, 151–158.
Middelboe, M., 2000. Bacterial growth rate and marine virus–host dynamics. Microb. Ecol. 40, 114–124.
Middleton, J.F., Bye, J.A.T., 2007. A review of the shelf-slope circulation along Australia's southern shelves: Cape Leeuwin to Portland. Prog. Oceanogr. 75, 1–41.
Middleton, J.F., Cirano, M., 2002. A northern boundary current along Australia's southern shelves: the Flinders Current. J. Geophys. Res. 107 (C9), 3129. http://dx.doi.org/10.1029/2000JC000701.
Middleton, J.F., Platov, G., 2003. The mean summertime circulation along Australia's southern shelves: a numerical study. J. Phys. Oceanogr. 33, 2270–2287.
Nieblas, A.E., Sloyan, B.M., Hobday, A.J., Coleman, R., Richardson, A.J., 2009. Variability of biological production in low wind-forced regional upwelling systems: a case study off southeastern Australia. Limnol. Oceanogr. 54, 1548–1558.
Paterson, J.S., Nayar, S., Mitchell, J.G., Seuront, L., 2012. A local upwelling controls viral and microbial community structure in South Australian continental shelf waters. Estuar. Coast. Shelf Sci. 96, 197–208.
Rochford, D.J., 1975. Nutrient enrichment of east Australian coastal waters. II* Laurieton Upwelling. Aust. J. Mar. Freshw. Res. 26, 233–243.
Rochford, D.J., 1977. A review of a possible upwelling situation off Port MacDonnell, SA. CSIRO Div. Fish. Oceanogr. 81, 1–17.
Roughan, M., Middleton, J.H., 2002. A comparison of observed upwelling mechanisms off the east coast of Australia. Cont. Shelf Res. 22, 2551–2572.
Ryther, J.H., 1969. Photosynthesis and fish production in the sea. Science 166, 72–76.
Schahinger, R.B., 1987. Structure of coastal upwelling events observed off the south-east coast of South Australia during February 1983–April 1984. Aust. J. Mar. Freshw. Res. 38, 439–459.
Servais, P., Casamayor, E.O., Courties, C., Catala, P., Parthuisot, N., Lebaron, P., 2003. Activity and diversity of bacterial cells with high and low nucleic acid content. Aquat. Microb. Ecol. 33, 41–51.
Seuront, L., Leterme, S.C., Middleton, J.F., Byrne, S., James, C., Luick, J., Nedoncelle, K., Paterson, J.S., Teixeira, C., van Dongen-Vogels, V., 2010. Biophysical couplings in South Australian shelf waters under conditions of summer upwelling and winter downwelling: results from the Southern Australia Integrated Marine Observing System (SAIMOS). In: Hall, J., Harrison, D.E., Stammer, D. (Eds.), Proceedings of the "*OceanObs '09: Sustained Ocean Observations and Information for Society*" Conference (Annex), Venice, Italy, 21–25 September 2009. ESA Publication WPP-306 (2010).
Sherr, E.B., Sherr, B.F., Wheeler, P.A., 2005. Distribution of coccoid cyanobacteria and small eukaryotic phytoplankton in the upwelling ecosystem off the Oregon coast during 2001 and 2002. Deep-Sea Res. II 52, 317–330.
Simpson, J.H., Bowers, D., 1981. Models of stratification and frontal movement in shelf seas. Deep-Sea Res. 28A, 727–738.
Smith, R.L., Huyer, A., Godfrey, S.J., Church, J.A., 1991. The Leeuwin Current off Western Australia, 1986–1987. J. Phys. Oceanogr. 21, 323–345.
Sommer, U., Stibor, H., Katechakis, A., Sommer, F., Hansen, T., 2002. Pelagic food web configurations at different levels of nutrient richness and their implications for the ratio fish production: primary production. Hydrobiologia 484, 11–20.
Suttle, C.A., Chen, F., 1992. Mechanisms and rates of decay of marine viruses in seawater. Appl. Environ. Microbiol. 58, 3721–3729.
Troncoso, V.A., Daneri, G., Cuevas, A.L., Jacob, B., Montero, P., 2003. Bacterial carbon flow in the Humboldt Current System off Chile. Mar. Ecol. Prog. Ser. 250, 1–12.
van Dongen-Vogels, V., Seymour, J.R., Middleton, J.F., Mitchell, J.G., Seuront, L., 2011. Influence of local physical events on picophytoplankton spatial and temporal dynamics in South Australian continental shelf waters. J. Plankton Res. 33, 1825–1841.
van Ruth, P.D., Ganf, G.G., Ward, T.M., 2010. Hot-spots of primary productivity: an alternative interpretation to conventional upwelling models. Estuar. Coast. Shelf Sci. 90, 142–158.
Wang, Y., Hammes, F., Boon, N., Chami, M., Egli, T., 2009. Isolation and characterization of low nucleic acid (LNA)-content bacteria. ISME J. 3, 889–902.
Weinbauer, M.G., 2004. Ecology of prokaryotic viruses. FEMS Microbiol. Rev. 28, 127–181.
Weinbauer, M.G., Bonilla-Findji, O., Chan, A.M., Dolan, J.R., Short, S.M., Šimek, K., Wilhelm, S.W., Suttle, C.A., 2011. *Synechococcus* growth in the ocean may depend on the lysis of heterotrophic bacteria. J. Plankton Res. 33, 1465–1476.
Winter, C., Herndl, G.J., Weinbauer, M.G., 2004. Diel cycles in viral infection of bacterioplankton in the North Sea. Aquat. Microb. Ecol. 35, 207–216.
Wommack, E.K., Colwell, R.R., 2000. Virioplankton: viruses in aquatic ecosystems. Microbiol. Mol. Biol. Rev. 64, 69–114.
Zar, J.H., 2009. Biostatistical Analysis, fifth ed. Prentice Hall, New Jersey.
Zubkov, M.V., Fuchs, B.M., Burkill, P.H., Amann, R., 2001. Comparison of cellular and biomass specific activities of dominant bacterioplankton groups in stratified waters of the Celtic Sea. Appl. Environ. Microbiol. 67, 5210–5218.
Zubkov, M.V., Burkill, P.H., Topping, J.N., 2007. Flow cytometric enumeration of DNA-stained oceanic planktonic protists. J. Plankton Res. 29, 79–86.

Please cite this article as: Paterson, J.S., et al., Population-specific shifts in viral and microbial abundance within a cryptic upwelling, J. Mar. Syst. (2013), http://dx.doi.org/10.1016/j.jmarsys.2012.12.009